Five-body van der Waals interactions

Jianing Han

Phys. Rev. A **95**, 062502 — Published 5 June 2017

DOI: 10.1103/PhysRevA.95.062502

Five-body van der Waals interactions

Jianing Han [*1]

[1]*Physics Department, University of South Alabama, Mobile, AL 36688.*

Abstract

We report on the five-body repulsive and attractive van der Waals interactions between the strongly dipole-dipole coupled Rydberg states. Compared to four-body van der Waals interactions, five-body van der Waals interactions show more energy levels and more potential wells caused by avoided crossings. This research bridges the few-body physics and many-body physics. Other disciplines, such as chemistry, biology, and medical fields, will also benefit from better understanding van der Waals interactions.

PACS numbers: 33.20.Bx, 36.40.Mr, 32.70.Jz

[*] Email address: jhan@southalabama.edu

Van der Waals interactions, discovered in 1870s, are dipole-dipole interactions, which can be calculated from the second order perturbation theory. Here dipoles can be electric dipoles or magnetic dipoles. In this article, we will focus on electric dipole-dipole interactions. Specifically, one-electron Rydberg atoms [1, 2] will be used as dipoles, because a one-electron Rydberg atom has an excited electron and an ion core, which are the two poles of an electric dipole. Therefore, the dipole-dipole interactions discussed in this article, specifically van der Waals interactions, refer to the interactions between Rydberg atoms.

Rydberg atoms are ideal candidates for studying van der Waals interactions for the following reasons. First, Rydberg atoms' radii are proportional to n^2, where n is the principal quantum number. Therefore, the dipole size can be adjusted by adjusting the principal quantum number. Second, as shown in this article, the van der Waals interaction strength depends on the energy difference, which is determined by the energy levels of Rydberg atoms. The energy levels of Rydberg atoms can be adjusted in two ways. First, those energy levels can be adjusted by adjusting the principal quantum number. Second, the energy levels of different angular momentum states of an atom with the same principal quantum number are different caused by the orbital polarization and orbital penetration of an atom with more than one electron. All of these features enable Rydberg atoms to be ideal candidates for studying van der Waals interactions.

The Rydberg-Rydberg molecules, bounded by dipole-dipole interactions, were first proposed by Christophe Boisseau et. al. [3]. The first experiment on Rydberg-Rydberg molecules was done by Farooqi et. al. [4] and then by Overstreet et. al. [5]. Recently, experiments were done on nearly resonant dipole-dipole coupled states, and a frequency shift, which was explained by a linear four-body model, has been observed [6]. The first repulsive van der Waals interaction measurement was done by Han et. al. [7]. In this article, we will continue to use the nearly degenerate and strongly dipole-dipole coupled states to study the five-body van der Waals interactions.

There are many applications about this research. In chemistry and chemical engineering, van der Waals interactions can be used to engineer molecules. In biology, van der Waals interactions can be used to modify cells or DNA. In medical fields, the van der Waals interactions can be used to synthesize medicine. Most importantly, the van der Waals interactions can be used in physics. For example, this research can also be applied to coherent radiation, such as superradiance, which is caused by phase locked dipole-dipole

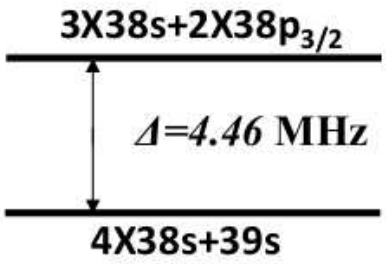

FIG. 1: The energy levels of the $4 \times 38s + 39s$ and $3 \times 38s + 2 \times 28p_{3/2}$. Here we again use the convention used in Ref. [19]. For instance, $4 \times 38s + 39s$ means all five atoms are far apart and they are not interacting with each other, while $38s38s38s38s39s$ means five atoms interact with each other through pairwise dipole-dipole interactions.

interactions [8–13]. Moreover, this study can be used to examine the ultracold plasma formation, especially the plasma formation of higher n states, which is led by the dipole-dipole collisions [14–17].

This paper is arranged in the following way: the five-body interaction theory is presented in the next section, which is followed by the discussions about the energy levels for different configurations.

In this article, 1D, 2D, and 3D five-body strongly dipole-dipole coupled Rydberg states will be investigated, and we will focus on $4\times38s+39s$ and $3\times38s+2\times28p_{3/2}$ states in ^{85}Rb. This approach can be generalized to solve other states and other elements. We continue to use the notation used in previous literatures [6, 18, 19]. Specifically, $4\times38s+39s$ means that when those five atoms are far apart or the interaction strength between atoms is negligible, four of the five atoms are in the $38s$ state and one of them is in the $39s$ state. We include all M states, where M is the projection of the total angular momentum of all five atoms along the z axis. In this article, we assume the probability in $4\times ns+(n+1)s$ states at $R\to\infty$ is one, where R is the internuclear spacing between two atoms. The energy difference between $4 \times 38s + 39s$ states and $3 \times 38s + 2 \times 28p_{3/2}$ states at $R = \infty$ is 4.46 MHz. as shown in Fig. 1 [6]. By the end of this article, the $4 \times 37s + 38s$ and $3 \times 37s + 2 \times 37p$ pair as well as $3 \times 40s + 2 \times 40p$ and $4 \times 40s + 41s$ pair are briefly discussed.

The way to accurately solve the five-body Rydberg problem is to solve the schrodinger equation of five electrons around five ion cores. If the density is low, the separation between

neighboring atoms, R, is large, the lowest order correction to the five-atom potential energy is the sum of all the pairwise dipole-dipole potential energies. The pairwise dipole-dipole interaction is shown in Eq. (1).

$$V_{12} = \frac{\vec{\mu}_1 \cdot \vec{\mu}_2 - 3(\vec{\mu}_1 \cdot \hat{R}_{12})(\vec{\mu}_2 \cdot \hat{R}_{12})}{R_{12}^3}, \tag{1}$$

where μ_1 and μ_2 are the dipole moments of atom 1 and atom 2 respectively. R_{12} is the internuclear spacing between atom 1 and 2. If there are five Rydberg atoms, the lowest order correction is the sum of ten pairs of dipole-dipole interactions as shown in Eq. (2) [20].

$$V_{12345} = V_{12} + V_{13} + V_{14} + V_{15} + V_{23} + V_{24} + V_{25} + V_{34} + V_{35} + V_{45}, \tag{2}$$

Let's start with the 3D configuration, and the 2D and 1D configurations can be derived by setting the angles to particular values. The 3D pairwise dipole-dipole interaction potential energy can be again expressed in terms of the spherical tensors. For instance, the pairwise dipole-dipole interaction between the atom located at position O and the atom located at position A as shown in Fig. 2 can be written as [21]:

$$\begin{aligned} V_{OA} = \frac{\mu_O \mu_A}{R_{OA}^3}\{ & -\frac{3}{2}\cos\theta_{OA}{}^2(e^{-2i\phi_{OA}}C_{1,1}^O C_{1,1}^A + e^{2i\phi_{OA}}C_{1,-1}^O C_{1,-1}^A) \\ & + \frac{1}{2}(C_{1,-1}^O C_{1,1}^A + C_{1,1}^O C_{1,-1}^A)(3\cos\theta_{OA}{}^2 - 2) + C_{1,0}^O C_{1,0}^A(1 - 3\sin\theta_{OA}{}^2) \\ & + \frac{3\sqrt{2}}{4}\sin(2\theta_{OA})[e^{-i\phi_{OA}}(C_{1,1}^O C_{1,0}^A + C_{1,0}^O C_{1,1}^A) - e^{i\phi_{OA}}(C_{1,-1}^O C_{1,0}^A + C_{1,0}^O C_{1,-1}^A)]\}, \end{aligned} \tag{3}$$

where $C_{k,q}$ is the normalized spherical tensor in Edmonds [22]. For instance, in the case of $k = 1$, or the first-order spherical tensor,

$$C_{1,0} = \frac{z}{r}, \tag{4}$$

$$C_{1,1} = \frac{-(x + iy)}{\sqrt{2}r}, \tag{5}$$

and

$$C_{1,-1} = \frac{x - iy}{\sqrt{2}r}. \tag{6}$$

θ_{OA} is the angle between OA and the xy plane, and ϕ_{OA} is the angle between the projection of OA on the xy plane and the x axis as shown in Fig. 2. If we set $\theta_{OA} = \frac{\pi}{2}$, and

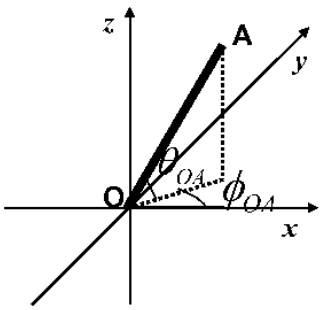

FIG. 2: Two dipoles, two Rydberg atoms in this case, are located at the two ends of a vector $\vec{OA}$, O and A.

$\phi_{OA} = 0$, the simplified potential is the 1D potential along the z axis, which is consistent with the equations given in other literatures [6]. From this equation, it can be proved that by switching the atom at the position O and the atom at the position A, the potential energy does not change, or

$$V_{OA} = V_{AO}. \tag{7}$$

All the calculations are done by directly diagonalizing the matrix, and no diabatization scheme has been used throughout the calculation.

If we set $\theta_{OA} = 0$, the potential is a potential in the xy plane. For example, if we set $\theta_{OA} = 0$, and $\phi_{OA} = 0$, the simplified potential is the 1D potential along the x axis. Here is another example: if we calculate the pairwise dipole-dipole potential for a pentagon in a plane as shown in Fig. 3(b), $\theta = 0$ for any one of the ten pairwise dipole-dipole potential energies.

We now discuss the calculated results. Fig. 4 shows the results for 1D, 2D, and 3D configurations plotted in Fig. 3. The right column of Fig. 4 is the corresponding magnified figure of the left column. For example, Fig. 4(a2) is the magnified figure of Fig. 4(a1). Figs. 4(a1) and (a2) are the energy levels of five atoms aligned along a straight line as shown in Fig. 3(a), or the 1D configuration. Figs. 4(b1) and (b2) are the energy levels of five atoms at the five corners of a pentagon on a plane or a 2D surface as shown in Fig. 3(b). Figs. 4(c1) and (c2) are the energy levels of five atoms at the five sites as shown in Fig. 3(c): four atoms are at the four vertices of a tetrahedron, and the fifth atom is at the center of this tetrahedron. This is a 3D configuration. From the energy levels of these three configurations in Fig. 3, the energy levels are more spread out as the dimension increases,

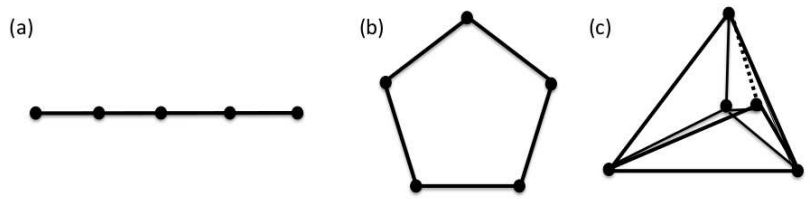

FIG. 3: (a) Five atoms aligned along a line (one-dimension or 1D configuration). (b) Five atoms are at the five vertices of a pentagon (2D configuration). (c) Three-dimension or 3D configuration. Four atoms are at the four corners of a tetrahedron, and the fifth atom is at the center of the tetrahedron.

which is caused by the fact that the atoms are closer to each other as the dimension increases. For example, the maximum distance in the 1D case is 4R, while the maximum distance in the 2D configuration is approximately 1.618R, where R is the distance between two closest neighboring atoms. The maximum distance in the 3D case is R. In addition, the maximum energy span increases due to the same reason.

Potential wells are formed in all three configurations. Fig. 5 shows the comparison of the potential wells formed in the 1D and 3D configurations. From Fig. 5(a), it is shown that potential wells can be formed through 1D five-body configurations. This has not been seen in the previous 1D calculations including two-body, three-body, and four-body calculations [18]. In addition, the 3D configuration clearly shows a much deeper potential well. From Fig. 5(b), it is shown that the 3D five-body van der Waals interactions can produce a potential well as deep as more than 1 MHz, which is about 20 times deeper than the deepest 1D five-body potential well. In addition, one can see that there are adiabatic avoided crossings and nonadiabatic crossings, or diabatic crossings. The size of the avoided crossing, or the energy difference between the states involved at the crossing point, shows the strength of the interaction between the coupled states. Specifically, greater energy spacing indicates greater interaction strength. To form a stable molecule, greater adiabatic avoided crossings are required. However, if we want greater forces, attractive van der Waals or repulsive van der Waals forces, diabatic crossings are preferred.

We now consider another pair of states, and we again consider the dipole-blockade case. Fig. 6 shows the five-body calculation for the following state, $4\times37s+38s$, which is strongly coupled with $3 \times 37s + 2 \times 37p$. The energy difference between those two states is about

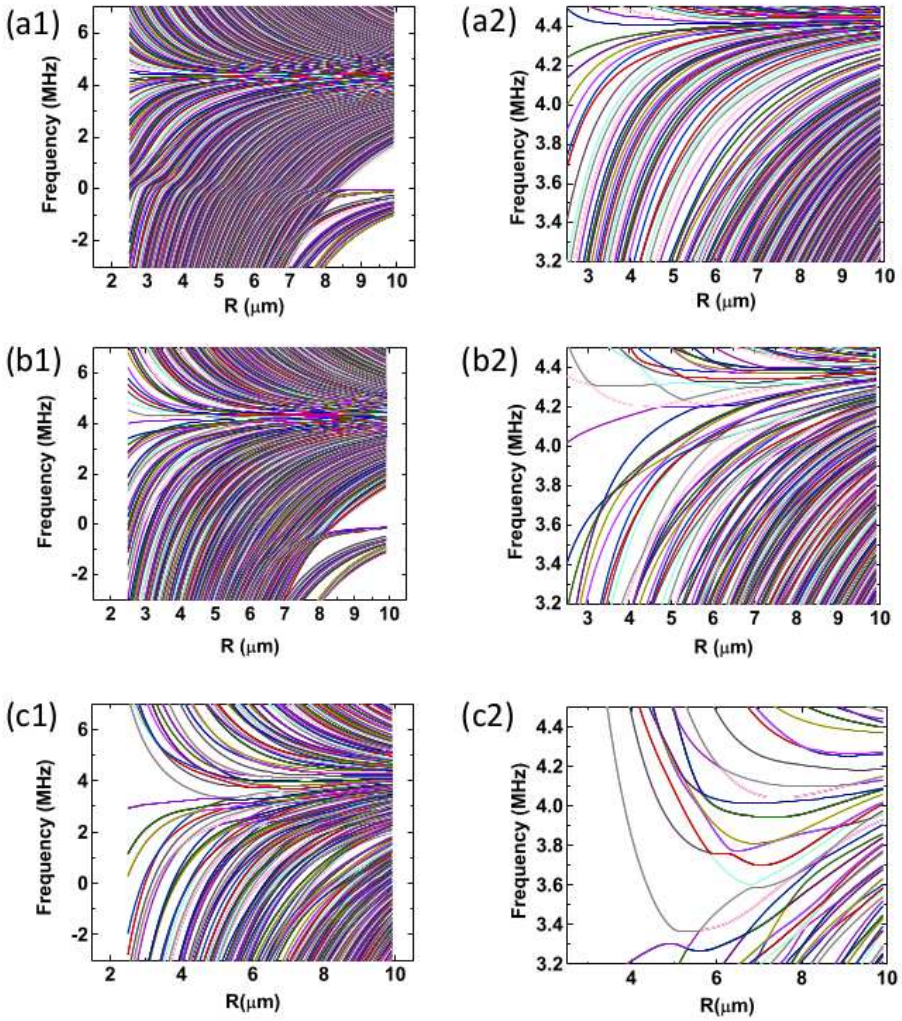

FIG. 4: (a1) and (a2) are the energy levels for the 1D five-body configuration as a function of the internuclear spacing R as shown in Fig. 3(a). (a2) is a portion of (a1). (b1) and (b2) are the energy levels for five atoms at the corners of a pentagon as shown in Fig. 3(b), and the length for each side of the pentagon is R. (b2) is a portion of (b1). (c1) and (c2) are the energy levels for five atoms: four atoms are on the four vertices of a tetrahedron and the fifth atom is at the center of the tetrahedron, and the length for each side of the tetrahedron is R as shown in Fig. 3(c). (c2) is a small portion of (c1).

103 MHz. In other words, the energy level of $3 \times 37s + 2 \times 37p$ is 103 MHz greater than the energy of $4 \times 37s + 38s$. Fig. 6(b) shows that the depth of the deepest potential is about 26 MHz, about a quarter of the energy spacing 103 MHz between the two coupled states, which is more than 20 times deeper than deepest potential well calculated for the $4 \times 38s + 39s$

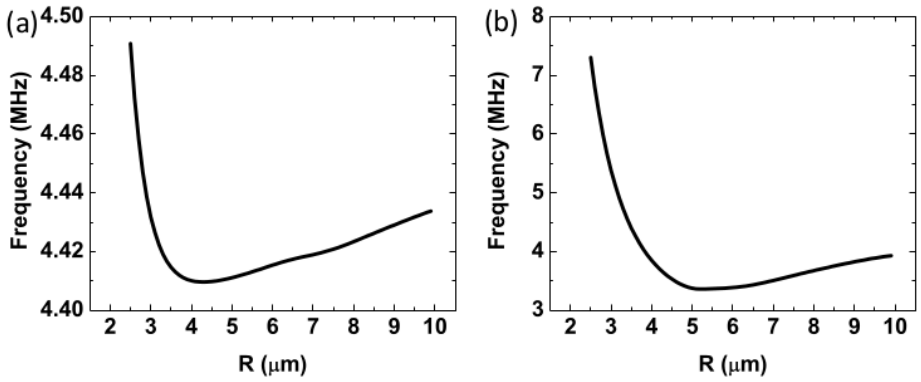

FIG. 5: (a) The deepest potential well in the 1D five-body configuration. (b) The deepest potential well in the 3D five-body configuration.

and $3 \times 38s + 2 \times 28p_{3/2}$ case. Compared the Fig. 4(c2) and Fig. 6(a), it is shown that both figures have similar structures, which is caused by the fact that the dipole moments in both cases are similar to each other, the only difference is the energy difference between the two coupled states. Previous discussions show that by increasing the dimension, the depth of the potential well will increase. This figure indicates that another way to form a deeper potential well is to increase the energy spacing between the coupled states. In addition, both Figs. 6 and 4 show that the potential wells are formed if the $3 \times ns + 2 \times np$ states are above the $4 \times ns + (n+1)s$. If both levels are reversed, the $4 \times ns + (n+1)s$ is above the $3 \times ns + 2 \times np$, a potential peak is expected, and this has been proved through numerical calculations. The interactions between $3 \times 40s + 2 \times 40p$ and $4 \times 40s + 41s$ have been calculated. The energy difference between that pair of states is -137 MHz. In other words, $4 \times 40s + 41s$ is 137 MHz above the $3 \times 40s + 2 \times 40p$ state. Fig. 7 shows the energy level with the highest peak among all energy levels. A potential peak can be used to stop atoms or investigate atom repulsion. In addition, a potential peak may be used to study quantum tunnelling.

In conclusion, it has been shown that 1D, 2D, and 3D five-body van der Waals interactions have been calculated. More than one MHz potential wells in certain configurations are observed for the 3D $4 \times 38s + 39s$ and $3 \times 38s + 2 \times 28p_{3/2}$ configuration. The potentials shown in Figs. 5 and 6(b) can be tested in ultracold atoms. We are also trying to generalize these models to room temperature atoms. Moreover, potential wells are observed for the 1D five-body calculation, which has not been seen in fewer-body 1D calculations. In addition, as

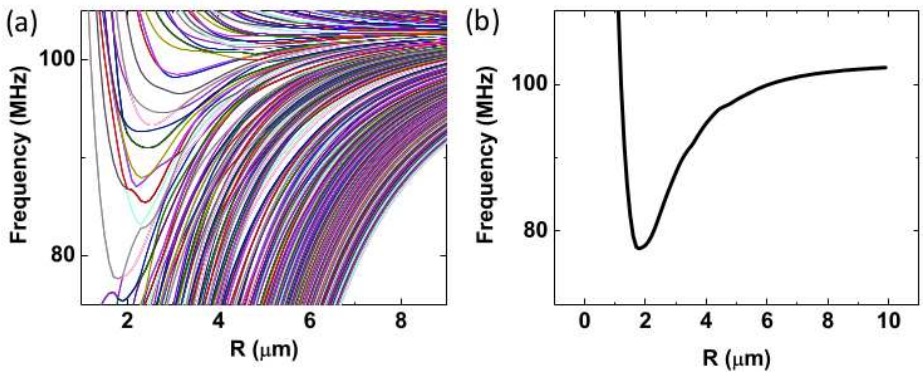

FIG. 6: (a) The energy levels calculated for the $3 \times 37s + 2 \times 37p$ coupled with $4 \times 37s + 38s$. (b) The deepest potential well in (a).

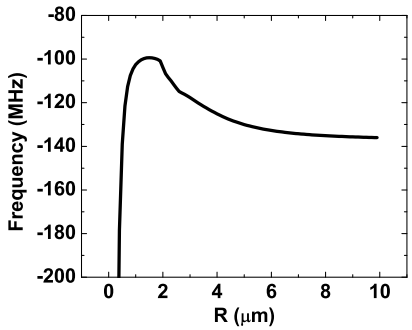

FIG. 7: One of the energy levels calculated for the $3 \times 40s + 2 \times 40p$ coupled with $4 \times 40s + 41s$.

the energy detuning increases, the depth of the potential wells increases. Moreover, potential peaks are observed for some energy levels.

It is a pleasure to acknowledge the support from the Army Research Office(ARO), the University of South Alabama Faculty Development Council (USAFDC), and the travel support from DOE/EPSCOR.

[1] T. F. Gallagher, Rydberg atoms. (Cambridge University Press, Cambridge, 1994).

[2] R. F. Stebbings, and F. B. Dunning, Rydberg States of Atoms and Molecules. (Cambridge University Press, Cambridge, 1983).

[3] Christophe Boisseau, Ionel Simbotin, and Robin Cote, Phys. Rev. Lett. **88**, 133004 (2002).

[4] S.M. Farooqi, D. Tong, S. Krishnan, J. Stanojevic, Y.P. Zhang, J.R. Ensher, A.S. Estrin, C.

Boisseau, R. Cote, E.E. Eyler, and P.L. Gould, Phys. Rev. Lett. **91**, 183002 (2003).

[5] K. R. Overstreet, Arne Schwettmann, Jonathan Tallant, and James P. Shaffer, Phys. Rev. A **76**, 011403(R) (2007).

[6] Jianing Han, Phys. Rev. A **84**, 052516(2011).

[7] J. Han, and T. F. Gallagher, Phys. Rev. A **77**, 015404(2009).

[8] R. H. Dicke, Phys. Rev. **93**, 99(1954).

[9] N. Skribanowitz, I. P. Herman, J. C. MacGillivray, and M. S. Feld, Phys. Rev. Lett. **30**, 309(1973).

[10] J. C. MacGillivray, and M. S. Feld, Phys. Rev. A **14**, 1169(1976).

[11] Q. H. F. Vrehen and H. M. Gibbs, Topics in Current Physics: Dissipative Systems in Quantum Optics (Springer, Berlin, Heidelberg, New York 1982).

[12] M. Gross and S. Haroche, Phys. Reports **93**, 301(1982).

[13] J. Han, and Haruka Maeda. Can. J. Phys. **92**, 1130 (2014).

[14] T. C. Killian, S. Kulin, S. D. Bergeson, L. A. Orozco, C. Orzel, and S. L. Rolston, Phys. Rev. Lett. **83**, 4776 (1999).

[15] T. F. Gallagher, P. Pillet, M. P. Robinson, B. Laburthe-Tolra, M. W. Noel, J. Opt. Soc. Am. B **20**, 1091 (2003).

[16] Wenhui Li, Michael W. Noel, Michael P. Robinson, Paul J. Tanner, Thomas F. Gallagher, Daniel Comparat, Bruno Laburthe Tolra, Nicolas Vanhaecke, Thibault Vogt, Nassim Zahzam, Pierre Pillet, and Duncan A. Tate, Phys. Rev. A **70**, 042713(2004).

[17] Paul J. Tanner, Jianing Han, E. S. Shuman, and T. F. Gallagher, Phys. Rev. Lett. **100**, 043002(2008).

[18] Jianing Han, Phys. Rev. A **82**, 052501(2010).

[19] Jianing Han, J. Phys. B **43** 235205(2010).

[20] J. von Stecher, J. P. D'Incao, and C. H. Greene, Nature Physics **5**, 417(2009).

[21] J. Han, and Chunyan Hu, Mol. Phys. **114**, 637 (2016).

[22] A. R. Edmonds, Angular Momentum in Quantum Mechanics (Princeton University Press, Princeton, New Jersey, 1957).